ORGANIC LETTERS

2012
Vol. 14, No. 13
3356–3359

Ambipolar Behavior of Hydrogen-Bonded Diketopyrrolopyrrole–Thiophene Co-oligomers Formed from Their Soluble Precursors

Yuki Suna,[†] Jun-ichi Nishida,[†] Yoshihide Fujisaki,[‡] and Yoshiro Yamashita*,[†]

Department of Electronic Chemistry, Interdisciplinary Graduate School of Science and Engineering, Tokyo Institute of Technology, G1-8, 4259, Nagatsuta, Midori-ku, Yokohama, Kanagawa, 226-8502, Japan, and NHK Science and Technology Research Laboratories, 1-10-11 Kinuta, Setagaya, Tokyo, 157-8510, Japan

yoshiro@echem.titech.ac.jp

Received May 15, 2012

ABSTRACT

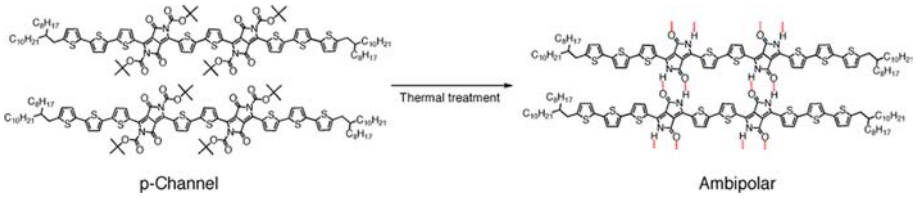

Organic field-effect transistors with hydrogen-bonded diketopyrrolopyrrole–thiophene co-oligomers were fabricated by a solution-process method with annealing at 200 °C, showing ambipolar charge-carrier transfer with field-effect mobilities up to $\mu_h = 6.7 \times 10^{-3}$ cm^2 V^{-1} s^{-1} and $\mu_e = 5.6 \times 10^{-3}$ cm^2 V^{-1} s^{-1}.

Solution-processable organic field-effect transistors (OFETs) have been desired for printing electronics.[1] a planar π-electron core and multiple hydrogen-bonding sites. For the past decade, DPP-based molecules and polymers have attracted much attention as electronic materials for OFETs[2] and OPVs.[3] Almost all of them have alkyl chains on their nitrogen atom to increase their solubility. In our previous work, we reported enhanced FET performances in thin-film transistors using DPPs with a hydrogen-bonding network.[4] However, their strong N–H···O=C hydrogen bonds make solution processes impossible.

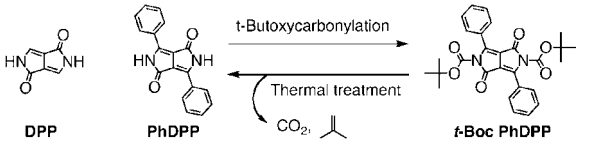

Figure 1. Chemical structures of DPP core, PhDPP, and its soluble precursor, *t*-Boc PhDPP.

DPP was originally developed as a high-performance organic pigment in the 1980s,[5] whereas its strong intermolecular interactions require a time- and energy-consuming dispersion step into the medium. In 1997, Iqbal et al.

[†] Tokyo Institute of Technology.
[‡] NHK Science and Technology Research Laboratories.

(1) Dimitrakopoulos, C. D.; Malenfant, R. L. *Adv. Mater.* **2002**, *14*, 99–117.
(2) (a) Fan, J.; Yuen, J. D.; Wang, M.; Seifer, J.; Seo, J.-H.; Mehebbi, A. R.; Zakhidov, D.; Heeger, A. J.; Wudl, F. *Adv. Mater.* **2012**, *24*, 2186–2190. (b) Chen, Z.; Lee, M. J.; Ashraf, R. S.; Gu, Y.; Akbert-Seifried, S.; Nielsen, M. M.; Schroeder, B.; Anthopoulos, T. D.; Heeney, M.; McMulloch, I.; Sirringhaus, H. *Adv. Mater.* **2012**, *24*, 647–652. (c) Lin, H.-W.; Lee, W.-Y.; Chen, W.-C. *J. Mater. Chem.* **2012**, *22*, 2120–2128. (d) Yuen, J. D.; Fan, J.; Seifter, J.; Lim, B.; Hufschmid, R.; Heeger, A. J.; Wudl, F. *J. Am. Chem. Soc.* **2011**, *133*, 20799–20807. (e) Wu, P.-T.; Kim, F.; Jenekhe, S. A. *Chem. Mater.* **2011**, *23*, 4618–4624. (f) Mohebbi, A. R.; Yuen, J.; Fan, J.; Munoz, C.; Wang, M. F.; Shirazi, R. S.; Wudl, F. *Adv. Mater.* **2011**, *23*, 4644–4648.
(3) Qu, S.; Tian, H. *Chem. Commun.* **2012**, *48*, 3039–3051.
(4) Suna, Y.; Nishida, J.; Fujisaki, Y.; Yamashita, Y. *Chem. Lett.* **2011**, *40*, 822–824.
(5) Wallquist, O.; Lenz, R. *Macromol. Symp.* **2002**, *187*, 617–629.

10.1021/ol3013364
Published on Web 06/20/2012

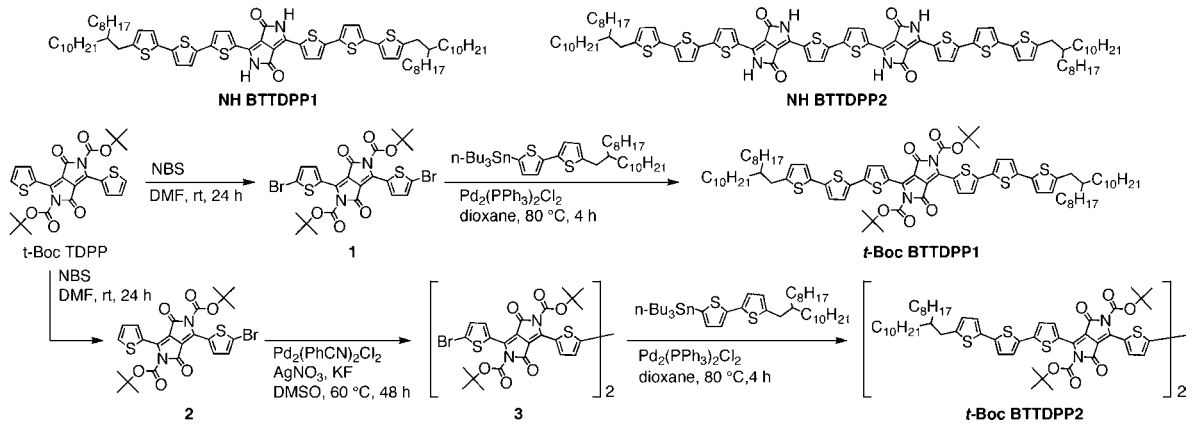

Figure 2. Chemical structures of DPP−thiophene co-oligomers **NH BTTDPP1** and **NH BTTDPP2** and synthetic procedure for their soluble precursors ***t*-Boc BTTDPP1** and ***t*-Boc BTTDPP2**.

demonstrated a method in which an insoluble DPP was converted into a soluble precursor by substitution of the NH group with a *tert*-butoxycarbonyl (*t*-Boc) group that can be eliminated at 180 °C. They succeeded in an in situ regeneration of an insoluble pigment in the application medium by thermal treatment.[6]

One example applying this system to FET has been reported on PhDPP,[7] in which an FET device with PhDPP was fabricated by thermal treatment after preparation of a spin-coated ***t*-Boc** PhDPP film. However, the gas components generated from thermal cleavage of *t*-Boc group (CO_2 and isobutene) disturbed the spin-coated film, resulting in hole mobility of 7.19×10^{-6} cm^2 V^{-1} s^{-1} which was lower than that in vapor-deposited film by 1 order of magnitude.

We have now designed DPP derivatives with thiophene rings, alkyl chains, and *t*-Boc groups. It was expected that an extended π-electron core enhances charge-carrier transfer, and long-branched alkyl chains and *t*-Boc groups increase solubility and give high quality films from their solution. In these films, thermally regenerated hydrogen-bonding networks are expected to strengthen intermolecular interactions. The effect of hydrogen bonds on the charge-carrier transfer behavior between hydrogen-bonded DPPs is discussed in this report.

***t*-Boc BTTDPP1** and ***t*-Boc BTTDPP2** with two DPP cores described in Figure 2 have been synthesized. ***t*-Boc BTTDPP1** was obtained by the Stille-coupling reaction of **1** with tributylstannyl bithiophene possessing a branched alkyl chain. In the case of ***t*-Boc BTTDPP2**, **2** was dimerized by palladium-catalyzed C−H homocoupling in the presence of the silver reagent prior to the Stille-coupling.[8] The details of the synthesis are given in Supporting Information.

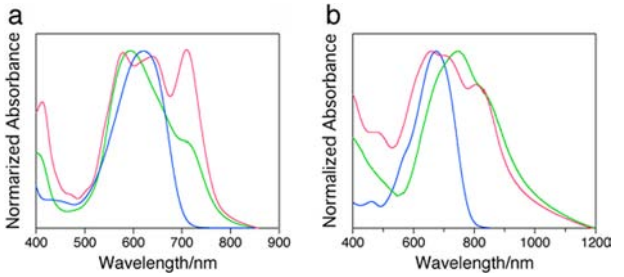

Figure 3. UV−vis-NIR absorption spectra of (a) ***t*-Boc BTTDPP1** and (b) ***t*-Boc BTTDPP2**. Blue: in $CHCl_3$ solution, green: as-cast film, red: annealed film.

Their UV−vis−NIR absorption spectra are shown in Figure 3. Thin films for this measurement were prepared on quartz plates by a drop-casting method from their $CHCl_3$ solutions (< 0.4 wt %). Thermal treatment of the films was performed on a hot plate at 200 °C for 30 min in air. In the solution, ***t*-Boc BTTDPP1** and ***t*-Boc BTTDPP2** have absorption maxima at 623 and 674 nm, respectively. In the film of ***t*-Boc BTTDPP1**, the onset wavelength is red-shifted by 80 nm compared with that in the solution. The shoulder peak at 711 nm observed in the as-cast film significantly increases and the vibronic structures appear in the annealed film. The onset wavelength of ***t*-Boc BTTDPP2** film is largely red-shifted from 800 nm in the solution to ca. 1000 nm. After annealing, the increase in absorbance at the shorter wavelength of 660 nm is much more remarkable than that at the shoulder peak of 808 nm. Such blue shifts are often

(6) Zambounis, J. S.; Hao, Z.; Iqbal, A. *Nature* **1997**, *388*, 131–132.
(7) Yanagisawa, H.; Mizuguchi, J.; Aramaki, S.; Sakai, Y. *Jpn. J. Appl. Phys.* **2008**, *47*, 4728–4731.
(8) Takahashi, M.; Masui, K.; Sekiguchi, H.; Kobayashi, N.; Mori, A.; Funahashi, M.; Tamaoki, N. *J. Am. Chem. Soc.* **2006**, *128*, 10930–10933.
(9) (a) Li, Z.; Zhang, Y.; Tsang, S.-W.; Du, X.; Zhou, J.; Tao, Y.; Ding, J. *J. Phys. Chem. C* **2011**, *115*, 18002–18009. (b) Brostein, H.; Chen, Z.; Ashraf, R. S.; Xhang, W.; Du, J.; Durrant, J. R.; Tuladhar, P. S.; Song, K.; Watkins, S. E.; Geerts, Y.; Wienk, M. M.; Janssen, R. A. J.; Anthopoulos, T.; Sirringhaus, H.; Heeney, M.; McColloch, I. *J. Am. Chem. Soc.* **2011**, *133*, 3272–3275. (c) Li, Y.; Sonar, P.; Singh, S. P.; Soh, M. S.; van Meurs, M.; Tan, J. *J. Am. Chem. Soc.* **2011**, *133*, 2198–2204. (d) Li, Y.; Singh, S. P.; Sonar, P. *Adv. Mater.* **2010**, *22*, 4862–4866.

observed in the films of donor−acceptor type DPP-based polymers. Polymer films exhibit blue-shifted absorption maxima compared with those in the solution, being considered to reflect ordered structures of polymers in the solid state.[2f,9] The blue shifts in these DPP derivatives also reflect the well-ordered structures of NH forms. Both DPP derivatives have no significant shift of onset wavelength upon annealing. The optical energy gaps estimated from the onset wavelength of **BTTDPP1** and **BTTDPP2** films were 1.59 and 1.24 eV, respectively, indicating that the energy gaps of the latter is lower than that of the former.

The thermal cleavage of *t*-Boc groups was confirmed by differential scanning calorimetry (DSC) measurements (Figure S1, Supporting Information). The DSC trace for the first heating cycle of ***t*-Boc BTTDPP1** showed an endothermic peak at 109 °C attributed to the phase transition caused by the alkyl chains. The second endothermic peak at 173 °C can be attributed to thermal decomposition of the *t*-Boc groups and disappeared from the second heating cycle. The temperature of the phase transition rose to 127 °C after the thermal decomposition of *t*-Boc groups. In ***t*-Boc BTTDPP2**, the thermal decomposition of the *t*-Boc groups was observed at 160 °C as a broad peak in the first heating cycle, while the phase transition of alkyl chains was not.

The IR spectra provided evidence for regeneration of the NH groups and formation of the hydrogen bonds of N−H···O=C (Figure S2, Supporting Information) upon thermal treatment. ***t*-Boc BTTDPP1** and ***t*-Boc BTTDPP2** showed two peaks assigned to free-carbonyl stretching vibration of the *t*-Boc and DPP core at 1741, 1684 cm^{-1} and 1749, 1683 cm^{-1}, respectively. After annealing, all of them disappeared, new peaks of hydrogen-bonded carbonyl groups appeared at 1640 cm^{-1}, and the peaks due to the regenerated NH groups were observed between from 2600 to 3200 cm^{-1}. Since regeneration of NH groups strengthens the intermolecular interaction, **NH BTTDPP1** and **NH BTTDPP2** became insoluble in common organic solvents.

Bottom-gate/bottom-contact FET devices using ***t*-Boc BTTDPP1** and ***t*-Boc BTTDPP2** as active layers were fabricated by a drop-casting method from their $CHCl_3$ solution. The measurements were carried out under vacuum, and their FET characteristics are summarized in Table 1. ***t*-Boc BTTDPP1** and ***t*-Boc BTTDPP2** showed

Table 1. Summary of FET Characteristics for DPP−Thiophene Co-oligomers

compd	μ^a ($cm^2V^{-1}s^{-1}$)	$I_{on}/I_{off}{}^b$	$V_{th}{}^c$ (V)
***t*-Boc BTTDPP1**	8.3×10^{-6} (h)	10^2	0
NH BTTDPP1	4.1×10^{-4} (h)	10	−25
	1.2×10^{-5} (e)	10	31
***t*-Boc BTTDPP2**	2.3×10^{-5} (h)	10^3	−15
NH BTTDPP2	6.7×10^{-3} (h)	10^2	−29
	5.6×10^{-3} (e)	10^2	36

[a] Field-effect mobility calculated from saturation regime. [b] Current on/off ratio. [c] Threshold voltage.

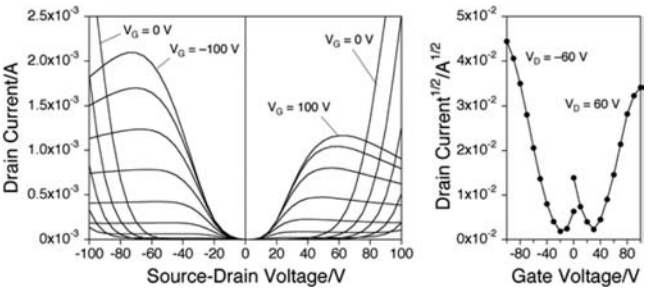

Figure 4. Output (left) and transfer (right) characteristic curves for **NH BTTDPP2**.

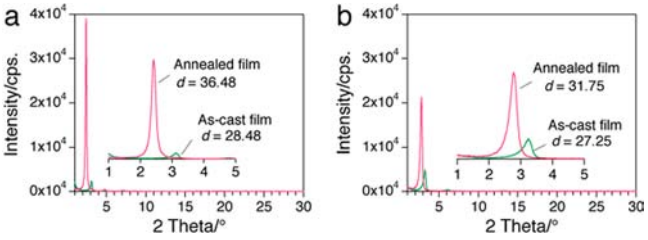

Figure 5. X-ray diffraction patterns for (a) **BTTDPP1** and (b) **BTTDPP2**; *t*-Boc form (green) and NH form (red).

low hole mobilities of 8.3×10^{-6} cm^2 V^{-1} s^{-1} and 2.3×10^{-5} cm^2 V^{-1} s^{-1}, respectively, which were enhanced upon annealing by 2 orders of magnitude. Although several DPP−thiophene molecules and their selenophene analogues have been reported as active materials for OFETs,[10] the reported FET properties on them are only p-type. Interestingly, the negative signs of charge carriers were observed in annealed devices of **NH BTTDPP1** and **NH BTTDPP2**. In particular, as shown in Figure 4, **NH BTTDPP2** exhibited well-balanced hole and electron mobilities of 6.7×10^{-3} cm^2 V^{-1} s^{-1} and 5.6×10^{-3} cm^2 V^{-1} s^{-1}, respectively. Similar changes have been reported in quaterrylene diimides, in which enhanced electron mobilities were also observed in hydrogen-bonded quaterrylene diimides after the thermal elimination of branched alkyl chains on their nitrogen atom.[11] In order to investigate the crystallinity and microstructures of the thin films, X-ray diffraction (XRD) measurements were carried out. As shown in Figure 5, the out-of-plane XRD patterns for the as-cast films have weak peaks at 3.10° in ***t*-Boc BTTDPP1** and 3.24° in ***t*-Boc BTTDPP2**. The intensities were significantly increased upon annealing at 200 °C, indicating well-ordered and dense packed crystalline structures

(10) (a) Mazzio, K. A.; Yuan, M. Y.; Okamoto, K.; Luscombe, C. K. *ACS Appl. Mater. Interfaces* **2011**, *3*, 271–278. (b) Tantiwiwat, M.; Tamayo, A.; Luu, N.; Dang, X.-D.; Nguyen, T.-Q. *J. Phys. Chem. C* **2008**, *112*, 17402.

(11) Oh, J. H.; Lee, W.-Y.; Noe, T.; Chen, W.-C.; Könemann, M.; Bao, Z. *J. Am. Chem. Soc.* **2011**, *133*, 4204–4207.

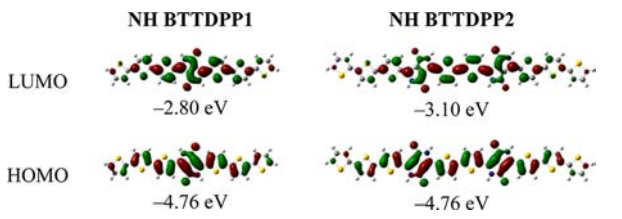

Figure 6. HOMO and LUMO surface plots of DPP–thiophene co-oligomers calculated with a DFT method at B3LYP/6-31G(d) level.

of **NH BTTDPP1** and **NH BTTDPP2** films. Furthermore, the *d*-spacing of these annealed films is elongated from 28.48 Å (2θ = 3.10°) to 36.48 Å (2θ = 2.42°) in **NH BTTDPP1** and from 27.25 Å (2θ = 3.24°) to 31.75 Å (2θ = 2.78°) in **NH BTTDPP2**. This indicates that the DPP–thiophene cores are less inclined to the substrate in the NH forms, which can be attributed to the formation of hydrogen bonds.

The geometry and electronic structures of **NH BTTDPP1** and **NH BTTDPP2** were calculated with a density functional theory (DFT) method at the B3LYP/6-31G(d) level using the Gaussian program 03. As shown in Figure 6, the HOMOs extend over the entire molecule, whereas the LUMOs are localized on the DPP core of **NH BTTDPP1** or between the two DPP cores and two thiophene rings of **NH BTTDPP2**. The HOMO energy levels of two **DPP** derivatives are the same level of −4.76 eV, whereas the LUMO energy level in **NH BTTDPP2** is lower than that in **NH BTTDPP1** by 0.3 eV. The increase of the number of electron accepting DPP core decreases the energy level of LUMO. In addition, the increase of hydrogen-bonding site in **NH BTTDPP2** would make intermolecular interactions more effective.

Photoelectron spectroscopy revealed that ***t*-Boc** and **NH BTTDPP1** films have almost the same HOMO energy levels of −5.28 eV. On the other hand, **NH BTTDPP2** has a lower energy level of −5.41 eV than that of *t*-Boc form (−5.20 eV). Hence, the LUMO energy levels estimated from the HOMO energy level and optical energy gaps are −3.69 eV in ***t*-Boc** and **NH BTTDPP1**, −3.96 eV in ***t*-Boc BTTDPP2**, and −4.17 eV in **NH BTTDPP2**. Decreasing the HOMO energy level in **NH BTTDPP2** film may be caused by strong intermolecular interactions.

In summary, we have synthesized two soluble precursors of DPP–thiophene co-oligomers and succeeded in fabricating FETs with their drop-casting films. The *t*-Boc groups could be subsequently removed by thermal treatment at 200 °C to regenerate NH forms. **NH BTTDPP2** with two electron-accepting DPP cores and four hydrogen-bonding sites showed well-balanced ambipolar behavior with hole and electron mobilities of 6.7×10^{-3} $cm^2 V^{-1} s^{-1}$ and 5.6×10^{-3} $cm^2 V^{-1} s^{-1}$, respectively. Hydrogen bonds between NH groups and adjacent carbonyl groups give highly ordered molecular arrangements in the films, resulting in changes of their electronic properties and FET behaviors.

Acknowledgment. This work was supported by a Grant-in-Aid for Scientific Research (No. 23350088 and 22550162).

Supporting Information Available. Details of the synthetic procedure, characterizations, DSC traces, IR spectra, output and transfer characteristic curves of FETs, and photoelectron spectra. This material is available free of charge via the Internet at http://pubs.acs.org

The authors declare no competing financial interest.